

# FLAT TERRAIN MEASUREMENTS AND PATH LOSS MODELS AT 1.0 AND 1.5 GHZ

Nektarios Moraitis\*, Panayiotis Frangos\*, Ileana Popescu\*, Alexandros Rogaris\*, and Seil Sautbekov\*\*

\* School of Electrical and Computing Engineering, National Technical University of Athens, 9, Iroon Polytechniou Str., 15773 Zografou, Athens, Greece.

\*\* Department of Physics and Technology, Al-Farabi Kazakh National University  
Almaty, Kazakhstan

E-mail: pfrangos@central.ntua.gr

(Selected from CEMA'24 Conference)

## Abstract

*In this paper an outdoor measurement campaign for almost flat terrain environment is undertaken for wireless mobile applications at frequencies 1.0 GHz and 1.5 GHz. The measured results are compared here both with the well – known in the literature “Two-Ray” (TR) model of wave propagation, as well as with the also well – known “Extended Hata” (EH) model. As a result, it is found here that under the conditions of this outdoor experiment the TR model is much more accurate, as compared to the measured results of ours. It is intended that further research by our research group will be conducted by our research group in the direction of comparison of our measured results with alternative analytical results which have been produced by us in previous publications of ours, in the “high frequency” regime.*

## 1. INTRODUCTION

The problem of electromagnetic (EM) wave propagation over the flat terrain (or over a lossy medium with flat interface) is well – known in the literature as the “Sommerfeld antenna radiation problem”, where the interest here is for observation points over the flat interface [1]-[23]. However, in this paper we concentrate in comparing our outdoor experimental measurements in “high frequency” regime (here for frequencies 1.0 GHz and 1.5 GHz), which are obtained here by our research group, with approximate or empirical models of electromagnetic (EM) wave propagation [24-30]. In near future proposed research by our group, we intend to compare our outdoor

experimental results measured by us here with alternative analytical results which have been produced by our research group in previous publications of ours (always in the “high frequency” regime).

This paper is organized as following: Section 2 describes the measurement equipment, as well as the procedure followed during our outdoor measurement campaign. Candidate path loss models to characterize the measured path loss are introduced and discussed in Section 3. Finally, conclusions and future research are presented in Section 4.

## **2. MEASUREMENT CAMPAIGN**

The measurements were carried out in a football (soccer) field inside our University (NTUA) campus, in order to represent a near flat earth scenario. The field was partially covered with grass, whereas it was surrounded by tall trees. Fig. 1 illustrates the measurement environment, as well as the transmit (Tx) and receive (Rx) locations. The red circles denote the two different Tx locations, being separated about 5 m, which concurrently transmit a continuous wave (CW) signal at 1.0 GHz (Tx1), and 1.5 GHz (Tx2), respectively. It is worth noticing that under such conditions no wave interference between the two transmitted EM waves, i.e., from the two transmitting antennas, is observed, because of the fact that both transmitted waves are very narrowband, since they are CW signals.

The two (2) antennas were both mounted at a height of 2.7 m about the field surface. Two signal generators were utilized to produce the transmitted signals, which were fed, through similar 3-m low loss cables, to similar vertically polarized omnidirectional antennas. They both have a half power beamwidth (HPBW) of  $45^\circ$  in the elevation plane and a constant gain of about 0.20 dBi in the azimuth plane at the selected frequencies. The transmitted effective isotropic radiated power (e.i.r.p.), was 16.1 dBm and 18.8 dBm, at 1.0 and 1.5 GHz, respectively.

An SRM-3006 frequency selective field meter by Narda GmbH (Pfullingen, Germany) in spectrum analysis mode was employed as the receiving unit. An electric field isotropic probe was used (420 MHz - 6 GHz with a 0 dBi gain), connected to the main control unit through a 1.5-m cable. The Rx sensor was mounted on a wooden tripod at 1.7 m above the field surface. The Rx unit recorded the power samples in dBm, using a

time average of 2 minutes. The Rx sensitivity was -120 dBm. The utilized Rx equipment was calibrated according to the ISO/IEC 17025:2017 standard [24]. Table I summarizes the Tx and Rx characteristics adopted in the launched measurement campaign.

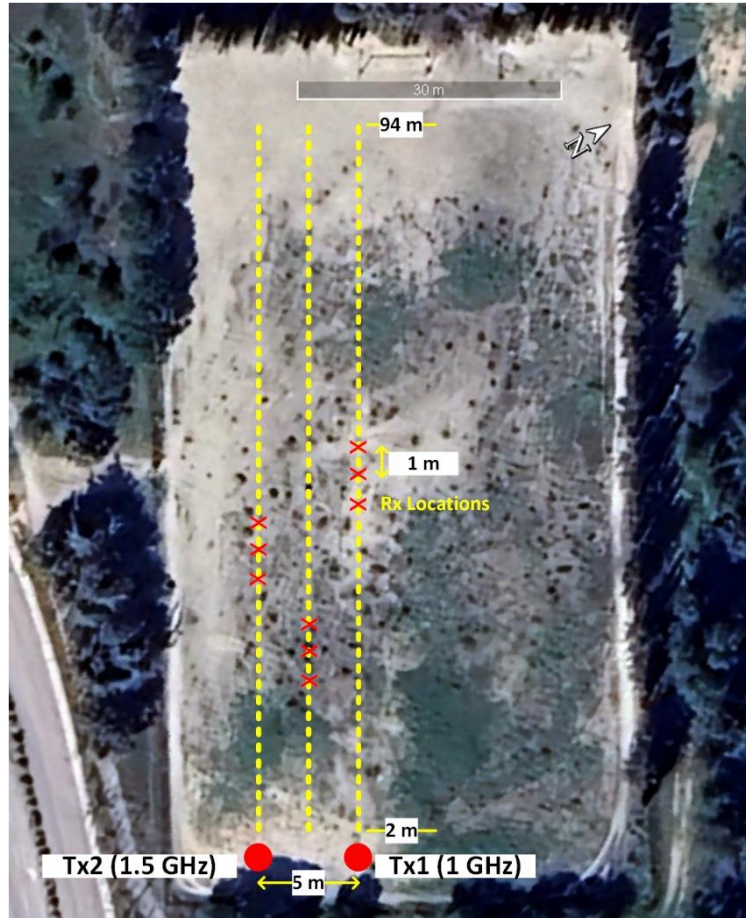


Figure 1. Measurement environment and locations.

Table 1. Transmitter and receiver characteristics during the measurement campaign at each selected frequency scenario.

	1.0 GHz	1.5 GHz
<b>Tx power [dBm]</b>	17	20
<b>Tx gain [dBi]</b>	0.20	
<b>Cable loss [dB]</b>	1.14	1.42
<b>EIRP [dBm]</b>	16.1	18.8
<b>Rx gain [dBi]</b>	0	
<b>Rx sensitivity [dBm]</b>	-120	

The Rx recorded the signal at distinct positions from 2 m up to 94 m in three (3) parallel routes, as also shown in Fig. 1, in steps of 1 m. At each measurement position the

Rx was stationary, having a line-of-sight (LOS) condition with the Tx. This entails a total number of 279 collected power samples at each frequency band.

Based on the received signal power the measured path loss PL, in decibels, at each Rx location can be described by:

$$PL = P_{Tx} - L_c + G_{Tx} + G_{Rx} - P_r \quad (1)$$

where  $P_{Tx}$  denotes the Tx power in dBm,  $L_c$  indicates the cable losses,  $G_{Tx}$ ,  $G_{Rx}$  stands for the Tx and Rx gains, respectively, in dBi, and  $P_r$  is the received signal power in dBm. Therefore, from (1), 279 path loss samples are resolved at each examined frequency scenario at a specific distance  $d_D$ , in meters, between Tx and Rx (length of the direct ray) that is given by:

$$d_D = \sqrt{d^2 + (h_t - h_r)^2} \quad (2)$$

where  $d$  indicates the horizontal (ground) distance, in meters, between Tx and Rx, and  $h_t$ ,  $h_r$  designate the Tx and Rx heights (2.7 and 1.7 m), respectively.

The raw data for both scenarios are shown in Fig. 2, where the received power versus distance is depicted. It should be pointed out that the distance from Tx in logarithmic scale, in meters, represents the direct distance ( $d_D$ ) between Tx and Rx.

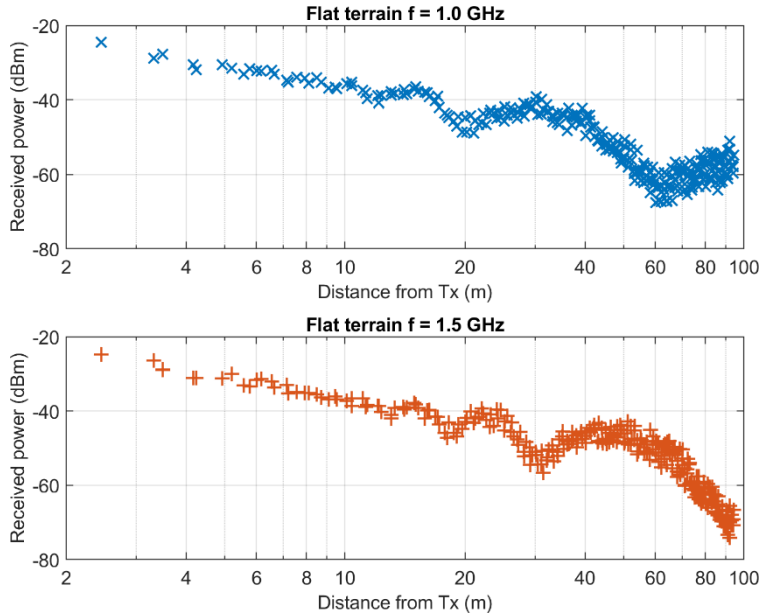


Figure 2. Received signal power at each measured location at 1 and 1.5 GHz.

Clearly the power samples imply a flat terrain pattern, where power drops are encountered at specific distances. This resembles to a two-ray pattern model, which will be examined for its appropriateness to model the measured path loss in Section 3, below, along with appropriate Extended Hata model, as well, for comparison purposes.

### 3. PATH LOSS MODELS RESULTS AND DISCUSSION

The two-ray model describes the signal propagation using two components. The direct ray between Tx and Rx and a ground reflected path ray. The path loss, in decibels, based on the two-ray model is given by [25]:

$$PL = 20 \log_{10} \left( \frac{4\pi d}{\lambda} \right) - 20 \log_{10} \left| 1 + \Gamma_V e^{j\Delta\varphi} \right| \quad (3)$$

where  $\lambda$  is the wavelength, in meters, at each selected frequency, and  $d$  is the ground (horizontal) distance between Tx and Rx, as previously mentioned. Furthermore,  $\Gamma_V$  denotes the vertical polarization reflection coefficient of the ground reflected path, and  $\Delta\varphi$  stands for the phase difference between the direct and the ground paths. The reflection coefficient is described by:

$$\Gamma_V = \frac{-\varepsilon_r \sin \theta_i + \sqrt{\varepsilon_r - (\cos \theta_i)^2}}{\varepsilon_r \sin \theta_i + \sqrt{\varepsilon_r - (\cos \theta_i)^2}} \quad (4)$$

where  $\theta_i$ , is the “grazing angle” of the incident wave (i.e., the angle between the incident EM wave and the flat terrain), and  $\varepsilon_r$  is the relative permittivity of the ground. Assuming a very dry ground,  $\varepsilon_r = 3$  according to [26]. Furthermore, the grazing angle in (4), is related to the geometrical propagation characteristics according to:

$$\begin{aligned} \sin \theta_i &= \left( \frac{h_t + h_r}{d_G} \right) \\ \cos \theta_i &= \left( \frac{d}{d_G} \right) \end{aligned} \quad (5)$$

where  $d_G$  denotes the length of the ground reflected ray, in meters, which can be calculated by:

$$d_G = \sqrt{d^2 + (h_t + h_r)^2} \quad (6)$$

Finally, the phase difference between of the path lengths between the direct and the ground reflected rays are given by:

$$\Delta\varphi = \frac{2\pi}{\lambda}(d_D - d_G) \quad (7)$$

where  $d_D$  and  $d_G$  are provided by (2) and (6), respectively.

Apart from the two-ray path loss model, the measured path loss is also compared with the “*Extended Hata*” model [27]. A rural/open area environment is assumed in this case; therefore, the path loss is given by:

$$PL = PL_U - 4.78(\log_{10}[\min\{\max\{150, f\}, 2000\}])^2 + 18.33\log_{10}[\min\{\max\{150, f\}, 2000\}] - 40.94 \quad (8)$$

where  $f$  is the operating frequency in MHz, and  $PL_U$  the path loss considering the urban environment. The latter parameter can be calculated according to:

$$PL_U = 46.3 + 33.9\log_{10}(2000) + 10\log_{10}(f / 2000) - 13.82\log_{10}(\max\{30, h_t\}) + (44.9 - 6.55\log_{10}(\max\{30, h_t\}))\log_{10}(d_D) - a(h_r) - b(h_t) \quad (9)$$

where  $d_D$  is the direct ray distance, converted in kilometres, between Tx and Rx, and  $f$  the operating frequency in MHz. Further,  $a(h_r)$  and  $b(h_t)$ , are the correction factors for the Rx and Tx, respectively, taking into account their specific heights  $h_r$  and  $h_t$  in meters. The correction factors are adopted for the rural/open area locations and can be calculated by:

$$b(h_t) = \min\{0, 20\log_{10}(h_t / 30)\} \quad (10)$$

and

$$a(h_r) = (1.1\log_{10}(f) - 0.7) \min\{10, h_r\} - (1.56\log_{10}(f) - 0.8) + \max\{0, 20\log_{10}(h_r / 10)\} \quad (11)$$

This model is widely used and is applicable for frequencies up to 3 GHz, and distances up to 40 km, respectively.

The results are presented in Fig. 3 where the path loss versus distance (in logarithmic scale) is provided along with the two different empirical models for comparison.

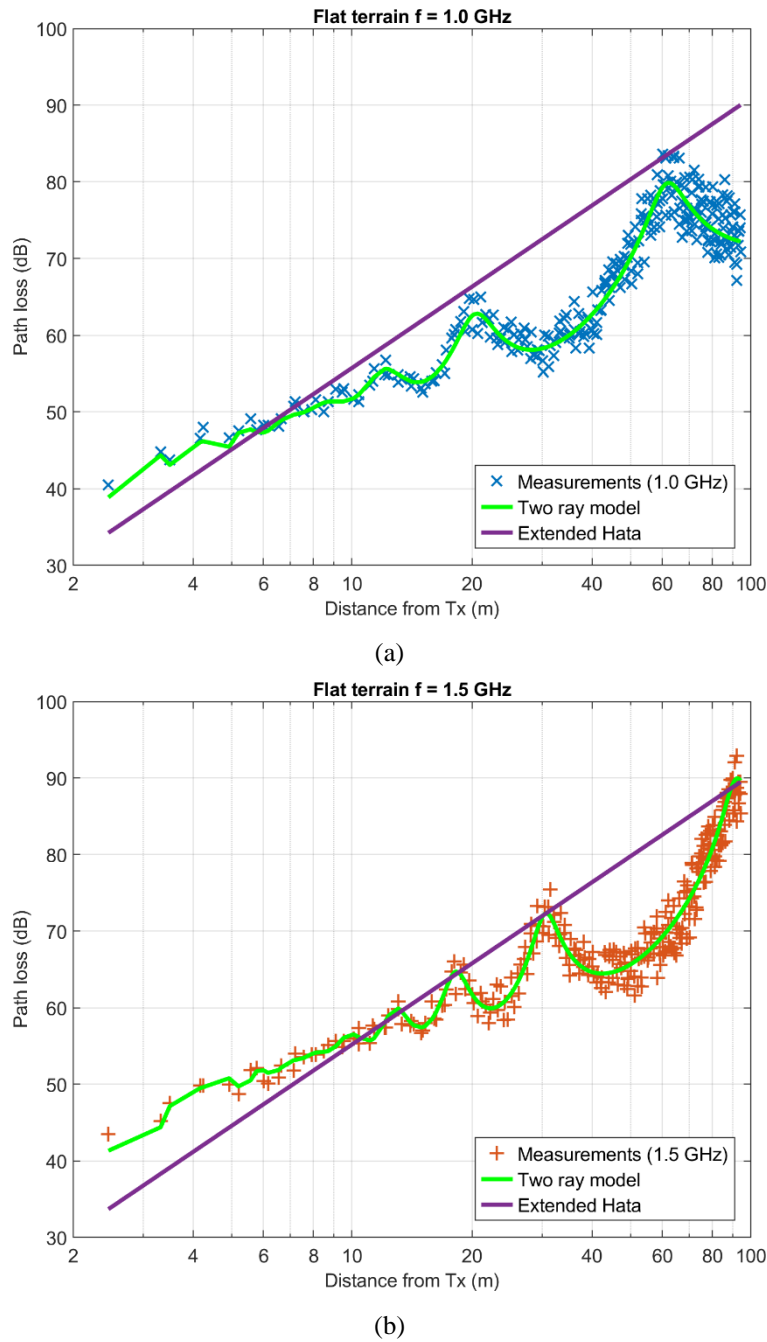


Figure 3. Path loss results versus distance. (a) 1.0 GHz. and (b) 1.5 GHz.

It is evident that “two-ray model” adapts better to the measured path loss, as it takes into account the geometrical characteristics of the propagating signal in the specific flat-terrain environment. On the other hand, the “Extended Hata model”, predicts well the path loss in the first few meters (about 10 m for 1.0 GHz measurements, or about 15 m, for 1.0 GHz measurements), but diverges afterwards compared to the measured samples.

To compare quantitatively and validate the realized outcome, appropriate error metrics are applied, in order to analyze the statistical error of each model [28], [29]. The mean absolute error (MAE), in decibels, is given by:

$$\text{MAE} = \frac{1}{N} \sum_{i=1}^N |PL_i^{\text{meas}} - PL_i^{\text{pred}}| \quad (12)$$

where  $PL_i^{\text{meas}}$  and  $PL_i^{\text{pred}}$  stand for the measured and predicted path loss values, respectively, and  $i$  is the index of the measured sample. Finally,  $N$  is the total number of path loss samples (279 at each frequency scenario). The mean absolute percentage error (MAPE) is calculated according to:

$$\text{MAPE} = \frac{1}{N} \sum_{i=1}^N \left| \frac{PL_i^{\text{meas}} - PL_i^{\text{pred}}}{PL_i^{\text{meas}}} \right| \times 100\% \quad (13)$$

Finally, the root mean square error (RMSE), which actually represents the shadow factor is given, in decibels, by:

$$\text{RMSE} = \sqrt{\frac{1}{N} \sum_{i=1}^N (PL_i^{\text{meas}} - PL_i^{\text{pred}})^2} \quad (14)$$

The prediction errors are computed in the following applying (12)-(14), for each assessed path loss model. An acceptable RMSE for a path loss model is 6-7 dB for urban locations, and higher than 10 up to 15 dB, for suburban and rural/open areas [30].

Table II summarizes the numerical results of the obtained error metrics for each model and frequency scenario.

Table 2. Statistical results between measured and predicted path loss for Two-Ray (TR) and Extended Hata (EH) models at each frequency scenario.

Model	Metric	1.0 GHz	1.5 GHz
<b>TR</b>	MAE [dB]	1.8	1.7
	MAPE [%]	2.6	2.4
	RMSE [dB]	2.3	2.1
<b>EH</b>	MAE [dB]	9.6	7.6
	MAPE [%]	14.4	11.3
	RMSE [dB]	10.8	9.1

The results in Table II reveal that “Two-Ray” (TR) model is better applicable in a near flat-terrain environment, that is much lower errors are obtained, as compared with the “Extended Hata” (EH) model. In terms of RMS error, TR model adjusts slightly

better at 1.0 GHz, nevertheless the error values between the two frequency scenarios are comparable. On the other hand, despite the high errors, EH model adapts better at 1.5 GHz, which implies that is more suitable at higher frequency applications over flat-terrain. However, at 1.0 GHz the results are discouraging, delivering an RMS error of 10.8 dB, which is higher than the acceptable value of 10 dB for rural/open areas, as suggested in [30].

Therefore, based on the above analysis, EH empirical model is not recommended for accurate path loss predictions in flat-terrain scenarios. Instead, geometrical optics (GO) models, such as “TR model”, are better applicable, providing accurate path loss predictions, thus being recommendable for such flat-terrain applications.

#### **4. CONCLUSION**

In this paper we presented an outdoor experimental measurement campaign of our research group from propagation of EM waves over flat terrain (at 1.0 GHz and 1.5 GHz) and compared the experimental results with the “two-ray” model, as well as with the “Extended Hata” propagation model. It was found that the former model (“two-ray” propagation model) provides very good accuracy to the measured data (as this might be expected in the “high frequency regime”, examined here).

As future work, the authors intend to assess additional path loss models of theirs (obtained by them through their previous research experience on EM propagation problems over the terrain), and validate their suitability to predict accurately the path loss in near flat-terrain scenarios.

#### **ACKNOWLEDGMENT**

The authors would like to thank the Kazakhstan Ministry of Education and Research for a research grant with title "AP19676900, The new technique for evaluation of the propagation of radio waves for terrestrial communications", which supported this research. In addition, they would like to thank Ph.D. candidate Mr. Basil Massinas (at NTUA) for his valuable help in the preparation of this paper.

## REFERENCES

- [1] A. N. Sommerfeld, “Propagation of waves in wireless telegraphy,” *Ann. Phys.*, 1909, 28, pp. 665-737.
- [2] K. A. Norton, “The propagation of radio waves over the surface of the earth and in the upper atmosphere,” *Proc. Inst. Radio Eng.*, vol. 24, no. 10, pp. 1367-1387, Oct. 1935. doi:10.1109/JRPROC.1936.227360.
- [3] A. K. Norton, “The propagation of radio waves over the surface of the earth and in the upper atmosphere,” *Proc. Inst. Radio Eng.*, vol. 25, no. 9, pp. 1203-1236, Sep. 1937. doi:10.1109/JRPROC.1937.228544.
- [4] J. Wait, “Launching a surface wave over the earth,” *Electron. Lett.*, vol. 3, no. 9, pp. 396-397, Sep. 1967. doi:10.1049/el:19670307.
- [5] R. J. King, “Electromagnetic wave propagation over a constant impedance plane,” *Radio Sci.*, vol. 4, no. 3, pp. 255-268, Mar. 1969. doi:10.1029/RS004i003p00255.
- [6] T. K. Sarkar, W. Dyab, M. N. Abdallah, M. Salazar-Palma, M. V. S. N. Prasad, S. W. Ting, and S. Barbin, “Electromagnetic macro modeling of propagation in mobile wireless communication: Theory and experiment,” *IEEE Antennas Propag. Mag.*, 2012, 54, pp. 17-43, doi:10.1109/MAP.2012.6387779.
- [7] J. G. V. Bladel, The Sommerfeld Dipole Problem. In *Electromagnetic Fields*, J. Wiley and Sons, Inc.: Hoboken, NJ, USA, 2007; Section 9.3, pp. 448–452.
- [8] G. Tyras, Field of a Dipole in a Stratified Medium. In *Radiation and Propagation of Electromagnetic Waves*; Academic Press, Inc., New York, NY, USA, 1969; Section 6, pp. 133–160.
- [9] Y. Rahmat-Samii, R. Mittra, P. Parhami, “Evaluation of Sommerfeld integrals for lossy half-space problems,” *Electromagnetics*, vol. 1, no. 1, pp. 1-28, 1981. doi:10.1080/02726348108915122.
- [10] R. E. Collin, “Hertzian dipole radiating over a lossy earth or sea: some early and late 20th-century controversies,” *IEEE Antennas Propag. Mag.*, 2004, vol. 46, no. 2, pp. 64-79, Apr. 2004. doi:10.1109/MAP.2004.1305535.
- [11] K. A. Michalski, “On the efficient evaluation of integral arising in the Sommerfeld halfspace problem,” *IEE Proc.-Microwaves, Antennas Propag.*, 1985, 132, pp. 312–318, doi:10.1049/ip-h-2.1985.0056.
- [12] G. Pelosi, J. L. Volakis, “On the centennial of Sommerfeld’s solution to the problem of dipole radiation over an imperfectly conducting half space,” *IEEE Antennas Propag. Mag.*, 2010, 52, pp. 198-201, doi:10.1109/MAP.2010.5586629.
- [13] J. R. Wait, “The ancient and modern history of EM ground-wave propagation,” *IEEE Antennas Propag. Mag.*, 1998, 40, pp. 7-24, doi:10.1109/74.735961.
- [14] A. Baños, *Dipole Radiation in the Presence of a Conducting Half-Space*, Pergamon Press, Oxford, UK, 1966; pp. 151–158.
- [15] S. S. Sautbekov, R.N. Kasimkhanova, and P. V. Frangos, “Modified solution of Sommerfeld’s problem,” in *Proc. CEMA’10 Conference*, Athens, Greece, 7–9 October 2010; pp. 5-8. Available online: [http://rcvt.tu-sofia.bg/CEMA/proceedings/CEMA\\_2010\\_proc.pdf](http://rcvt.tu-sofia.bg/CEMA/proceedings/CEMA_2010_proc.pdf) (accessed on May 2021).
- [16] S. Sautbekov, “The generalized solutions of a system of Maxwell’s equations for the uniaxial anisotropic media,” in *Electromagnetic Waves Propagation in Complex Matter*; IntechOpen Limited: London, UK, 2011; Chapter 1, pp. 1–24, doi:10.5772/16886.

- [17] K. Ioannidi, C. Christakis, S. Sautbekov, P. Frangos, and S. K. Atanov, "The radiation problem from a vertical Hertzian dipole antenna above flat and lossy ground: Novel formulation in the spectral domain with closed-form analytical solution in the high frequency regime," *Int. J. Antennas Propag. (IJAP)*, 2014, Special Issue on 'Propagation of Electromagnetic Waves in Terrestrial Environment for Applications in Wireless Telecommunications', doi:10.1155/2014/989348.
- [18] S. Bourgiotis, K. Ioannidi, C. Christakis, S. Sautbekov, P. Frangos, "The radiation problem from a vertical short dipole antenna above flat and lossy ground: Novel formulation in the spectral domain with numerical solution and closed-form analytical solution in the high frequency regime," in Proc. CEMA'14 Conference, Sofia, Bulgaria, 16–18 October 2014; pp. 12–18, Available online: [http://rcvt.tu-sofia.bg/CEMA/proceedings/CEMA\\_2014\\_proc.pdf](http://rcvt.tu-sofia.bg/CEMA/proceedings/CEMA_2014_proc.pdf) (accessed on May 2021).
- [19] S. Bourgiotis, A. Chrysostomou, K. Ioannidi; S. Sautbekov, and P. Frangos, "Radiation of a vertical dipole over flat and lossy ground using the spectral domain approach: Comparison of stationary phase method analytical solution with numerical integration results," *Electronics and Electrical Engineering Journal*, 2015, 21, pp. 38-41, doi:10.5755/j01.eee.21.3.10268.
- [20] A. Chrysostomou, S. Bourgiotis, S. Sautbekov, K. Ioannidi, and P. Frangos, "Radiation of a vertical dipole antenna over flat and lossy ground: Accurate electromagnetic field calculation using the spectral domain approach along with redefined integral representations and corresponding novel analytical solution," *Electronics and Electrical Engineering Journal*, 2016, 22, pp. 54–61, doi:10.5755/j01.eie.22.2.14592.
- [21] S. Sautbekov, S. Bourgiotis, A. Chrysostomou, and P. Frangos, "A novel asymptotic solution to the Sommerfeld radiation problem: Analytic field expressions and the emergence of the surface waves," *PIER M*, 2018, 64, pp. 9–22, doi:10.2528/PIERM17082806.
- [22] S. Bourgiotis, P. Frangos, S. Sautbekov and M. Pshikov, "The Evaluation of an asymptotic solution to the Sommerfeld radiation problem using an efficient method for the calculation of Sommerfeld integrals in the spectral domain," *Electronics Journal*, MDPI Publisher, 1, <https://doi.org/10.3390/electronics1010000>, <https://www.mdpi.com/journal/electronics>, Special Issue on 'Propagation of Electromagnetic Waves in Terrestrial Environment for Applications in Wireless Telecommunications and Radar Systems', June 2021.
- [23] J. Fikioris, *Introduction to Antenna Theory and Propagation of Electromagnetic Waves*. National Technical University of Athens: Athens, Greece, 1982. (In Greek).
- [24] International Organization for Standardization, "General requirements for the competence of testing and calibration laboratories," ISO/IEC 17025:2017, Geneva, Switzerland, Nov. 2017.
- [25] T. S. Rappaport, *Wireless Communications: Principles and Practice*. (2nd ed.), Prentice Hall, Upper Saddle River, New Jersey, 2002.
- [26] Electrical Characteristics of the Surface of the Earth, document ITU-R P.527-6, International Telecommunication Union, Geneva, Switzerland, Sep. 2021.

- [27] Monte Carlo simulation methodology for the use in sharing and compatibility studies between different radio services or systems, document ITU-R SM.2028-2, International Telecommunication Union, Geneva, Switzerland, Jun. 2017.
- [28] E. Östlin, H. J. Zepernick, and H. Suzuki, “Macrocell path-loss prediction using artificial neural networks,” *IEEE Trans. Veh. Technol.*, vol. 59, no. 6, pp. 2735-2747, Jul. 2010.
- [29] Y. Zhang, et al., “Path loss prediction based on machine learning: Principle, method, and data expansion,” *Appl. Sci.*, vol. 9, no. 9, pp. 1-18, May 2019.
- [30] J. D. Parsons, *The Mobile Radio Propagation Channel*. 2nd ed., New York: Wiley, 2000.